CASE REPORT

Precision and Future Medicine 2020;4(2):75-80
https://doi.org/10.23838/pfm.2020.00086
pISSN: 2508-7940 · eISSN: 2508-7959

PRECISION AND FUTURE MEDICINE

Three-dimensional reconstruction of the facial nerve course in parotid gland tumor using double echo steady state with water-excitation magnetic resonance images

Yong Gi Jung[1], Yi-Kyung Kim[2], Hyung-Jin Kim[2], Han-Sin Jeong[1]

[1]Department of Otorhinolaryngology Head and Neck Surgery, Samsung Medical Center, Sungkyunkwan University School of Medicine, Seoul, Korea
[2]Department of Radiology, Samsung Medical Center, Sungkyunkwan University School of Medicine, Seoul, Korea

Received: May 7, 2020
Revised: May 28, 2020
Accepted: May 29, 2020

Corresponding author:
Han-Sin Jeong
Department of Otorhinolaryngology Head and Neck Surgery, Samsung Medical Center, Sungkyunkwan University School of Medicine, 81 Irwon-ro, Gangnam-gu, Seoul 06351, Korea
Tel: +82-2-3410-3579
E-mail: hansin.jeong@gmail.com

ABSTRACT

Functional preservation of the facial nerve (FN) is essential in parotid tumor surgery. Recently, direct visualization of the FN in the parotid gland (double-echo steady-state sequence with water excitation magnetic resonance imaging [DESS-WE-MRI]) has been attempted with promising diagnostic accuracy. In this report, we present three-dimensional (3D) reconstruction of the FN course in two parotid gland tumor cases using DESS-WE-MRI images for the first time. One patient had a recurrent benign parotid gland tumor, while the other patient had a malignant parotid gland tumor. Regions-of-interest including the FN and the tumors were manually selected in each section of the DESS-WE-MRI images. The 3D renderings were then created with an In-Vesalius software. The FNs were well-demarcated to the temporofacial and cervicofacial branches. This virtual reconstruction of the FN nerve course can provide comprehensive and immediate understanding of the anatomical relationship between tumor and the FN, even for surgeons unaccustomed with DESS-WE-MRI images.

Keywords: Facial nerve; Magnetic resonance imaging; Neoplasms; Parotid gland; Surgery

INTRODUCTION

Tumors (benign or malignant) arising from the parotid gland are not common, with an incidence of five to six per 100,000 in the population [1]. Primary treatment for parotid gland tumors is complete surgical removal for several reasons including continuous growth of the tumor, lack of effective medical treatment, difficulty in differentiating between benign and malignant tumors, and the potential for malignant transformation in a subset of benign tumors [2]. The surgical goal of parotid gland tumors is complete removal of the tumors without complications [2]. Among the potential complications associated with parotid gland surgery, facial nerve weakness is the most disturbing, resulting in a severely lowered patient quality of life [2,3].

Even with various techniques (described below), 14% to 64% of parotidectomy cases suffer facial nerve weakness postoperatively [4-6]. For small and superficial tumors in the parotid gland, the risk of facial nerve weakness is not high (less than 5% with an experienced surgeon) [3]. However, its incidence has increased dramatically (up to 30%) in large tumors, deep seated tumors, revision surgery, and malignant tumors (requiring more extensive surgical dissection of the parotid gland) [7].

During parotidectomy, several measures have been commonly used to prevent or minimize facial nerve injury [8,9]. Surgical landmarks (tympanomastoid suture line, tragal point and the posterior belly of the digastric muscles) consistently indicate the facial nerve trunk, which is the starting point of antegrade facial nerve dissection [8,9]. Most surgeons use surgical magnification in parotid gland surgery (surgical loupes or microscopes). In addition, intraoperative monitoring of the facial nerve greatly helps surgeons identify the facial nerve [4,5].

With the advancement of imaging tools, preoperative computed tomography (CT) or magnetic resonance imaging (MRI) images can delineate and locate tumors in the parotid gland, and estimate the anatomical relationship between the tumor and the facial nerve [10-12]. Typically, the relative location of the tumor to the facial nerve plane (superficial or deep seated tumor) can be predicted preoperatively by indirect methods using a facial nerve line or retro-mandibular vein line [11]. Recently, direct visualization of the peripheral nerve and facial nerve has been attempted with improved accuracy of localization using particular sequences of MRIs to enhance visualization of the peripheral nerve [13,14]. Among the methods, double-echo steady-state sequence with water excitation MRI (DESS-WE-MRI) is one promising tool that can directly visualize the peripheral nerves in various regions [13,14]. Our data (unpublished) and those of other studies show that DESS-WE-MRI of the parotid gland can visualize the facial nerve around parotid gland tumors accurately [15].

In this report, we present two cases of virtual reconstruction of the three-dimensional (3D) anatomy of the facial nerve course around parotid gland tumors using DESS-WE-MRI images, for the first time. It can provide opportunities to the surgeon for better surgical planning and better preservation of the facial nerve during parotidectomy.

CASE REPORT

In this report, we present two patients with parotid gland tumor, who underwent parotidectomy. Both patients exhibited no facial weakness at presentation. The study protocol was previously approved (IRB file no. 2017-07-084-003, ClinicalTrials.gov ID NCT03822728), and all patients submitted written informed consent.

The first patient was a 50-year-old man with a recurred mass in his right parotid gland. Twenty years prior, he had undergone surgery for a benign tumor in his right parotid gland. CT scans revealed a 3-cm-sized benign looking tumor. Aspiration cytology suggested a pleomorphic adenoma. An MRI examination including the DESS-WE sequence was performed, and the patient underwent superficial parotidectomy with preservation of all facial nerve branches. The final pathology revealed a 3.3-cm-sized tumor that proved to be a pleomorphic adenoma with clear resection margins.

The second patient was a 30-year-old man with a tumor in his left parotid gland. The tumor was suspected to be a malignant tumor from preoperative cytology and CT images. Based on the findings of the initial work-ups, positron emission tomography with CT and DESS-WE-MRI scans were performed, and no metastasis was found. The patient underwent complete parotidectomy with preservation of the facial nerve and prophylactic neck dissection. The final pathology revealed a 4.0-cm-sized mucoepidermoid carcinoma with extraparenchymal extension and no lymph node metastasis (pT3N0).

The two patients were discharged home uneventfully at postoperative day 7. No facial weakness was observed postoperatively.

MRI images and interpretation

All MRI examinations were performed with a Siemens Skyra 3-T scanner using a 20-channel head and neck coil. After obtaining conventional spin-echo T1-weighted images and fat-suppressed T2-weighted images, the 3D-DESS-WE sequences were obtained (repetition time/echo time/number of excitation, 13.62 ms/5 ms/1; flip angle, 30°; field-of-view, 200 × 200 mm; matrix, 384 × 230; effective section thickness, 0.5 mm; slab thickness, 10.4 cm; acquisition time, 4 minutes 35 seconds). Finally, contrast-enhanced axial and coronal spin-echo T1-weighted images with fat suppression were obtained after intravenous injection of 0.1 mmol/kg of gadolinium-based contrast material.

The MRI images were evaluated by two neuro-radiologists (YKK, HJK) with more than 5 years of head and neck MRI interpretation experience. On axial DESS-WE-MRI images, we evaluated the visibility of the main trunk, temporofacial division, and cervicofacial division of the intraparotid facial

nerve on the affected side. MRI interpretation was performed independently and any ambiguity was solved by a joint consensus. To avoid any potential misinterpretation of the ductal/vascular structures for neural structures, we focused on the continuity of the facial nerve and followed its course along the intra-temporal and extra-mastoid segments. Once the nerve penetrated the posterior capsule of the parotid gland, it was traced anteriorly. In addition, the tumor location in relation to the entire range of the visible facial nerve from the main trunk to its divisional branches was determined on the reformatted 3 mm thick axial, sagittal, and coronal DESS-WE images.

3D visualization of the parotid tumor and facial nerve: technical notes

Digital Imaging and Communications in Medicine (DICOM) format data of the axial images were extracted from the MRI scans of the two patients. The 3D model, including the tumor and the facial nerve, was fabricated using InVesalius 3.3.1 (CTI, Sao Paulo, Brazil) software, and the model was exported in the Standard Triangle Language (STL) format. The Meshmixer 3.5 program (Autodesk, San Rafael, CA, USA) was used to remove unnecessary parts of the 3D model, and Zbrush 2020 (Pixologic, Los Angeles CA, USA) was used to smoothly trim the surface. Finally, 3D-Coat (www.3dcpat.com) was used to texture the facial nerve and tumor. Mandible and lateral skull base were also reconstructed and 3D visualized from the information of MRI images for anatomic orientation of the facial nerve and parotid tumors (Fig. 1).

Surgical findings and 3D reconstructed images

In the first case, the tumor was located in the superficial lobe of the parotid gland at the level of the facial nerve trunk. The facial nerve branched off just before the tumor, and the temporofacial and cervicofacial branches ran superiorly and inferiorly over the surface of the tumor. The tumor was well-demarcated from the parotid gland. However, antegrade dissection of the facial nerve trunk from the tumor was not easy because of fibrosis from a previous surgery. The two main branches were further divided into five peripheral branches, deep to the tumor, at the anterior boundary of the tumor. The tumor was resected safely with some surrounding parotid gland tissues and all the branches were preserved during surgery. DESS-WE-MRI and 3D reconstructed models clearly visualized the mastoid portion of the facial nerve, the facial nerve trunk (extra-mastoid portion), and the two main branches (Fig. 2A).

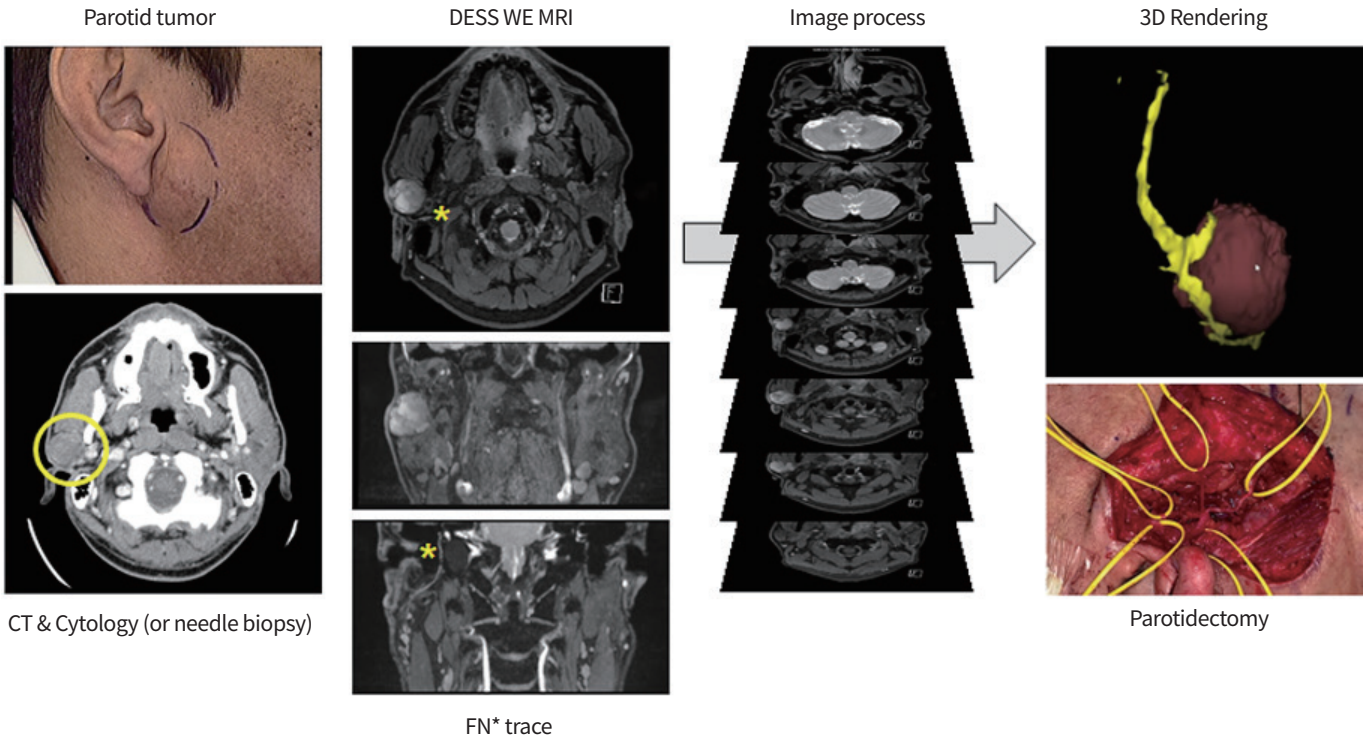

Fig. 1. Overview of this case presentation and imaging process for three-dimensional visualization of the facial nerve (FN; asterisks) course around the parotid tumor (yellow circle: right parotid gland tumor). DESS-WE-MRI, double-echo steady-state sequence with water excitation magnetic resonance imaging; CT, computed tomography.

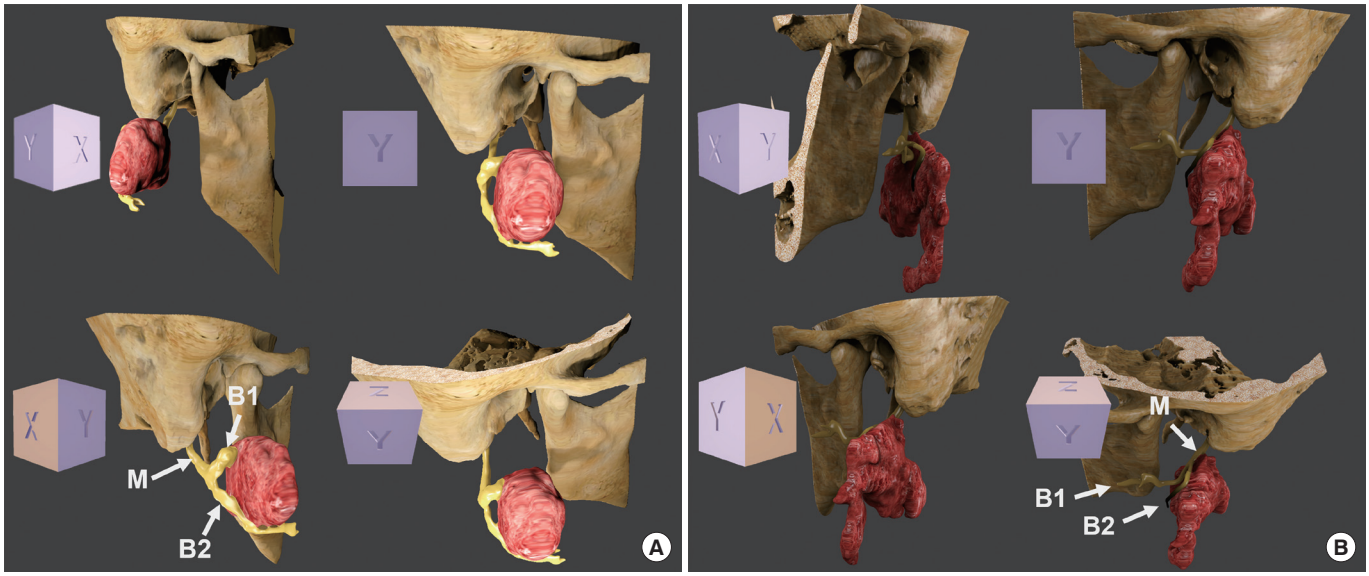

Fig. 2. Integrated three-dimensional model of the facial nerve and parotid gland tumor. (A) Case 1, (B) Case 2. M, main trunk of the facial nerve; B1, temporofacial branch; B2, cervicofacial branch.

In the second case, the tumor was located in the inferior portion of the left parotid gland, spreading across the facial nerve plane (superficial and deep lobes). The tumor border was not clearly defined. The facial nerve trunk and the cervicofacial branch ran horizontally just on the superior surface of the tumor. At the anterior end of the tumor, the cervicofacial branch coursed inferiorly. Tumor invasion into the facial nerve was not observed, although the cervicofacial branch closely adhered to the superior surface of the tumor. Fortunately, all the branches of the facial nerve were separated safely from the tumor, and the tumor was removed cleanly with a minimal surgical safety margin superiorly (2 to 3 mm). The anatomical relationship of the extra-mastoid facial nerve, the two main branches and the tumor in the 3D reconstructed model was in full accord with the surgical findings (Fig. 2B).

DISCUSSION

Functional preservation of the facial nerve is one of the essential surgical goals for most tumors in the parotid gland, except for cases with some malignancies or preoperative facial nerve palsy [2]. The incidence of postoperative facial weakness is low, and for superficial or small benign parotid gland tumors, the number does not go beyond 5% of cases (2% to 4%) [7]. However, there is still room for improvement for cases with malignant tumors or recurrent diseases, representing nearly 15% to 30% of facial weakness cases after surgery [7]. In addition to surgical magnification and intra-operative facial nerve monitoring [4,5], preoperative prediction of parotid tumors and the facial nerve course with an understanding of their anatomical relationship seems helpful for surgical planning [7].

To further improve the outcome of facial nerve complications, we have attempted a direct visualization of the facial nerve using DESS-WE-MRI images in complicated cases, such as tumors large enough to involve the deep lobe of the parotid gland, tumors suspicious for malignancy and recurrent tumors requiring revision parotid surgery [7]. One step further, we presented 3D reconstruction of the facial nerve around parotid tumors in this report, using DESS-WE-MRI images. We believe that this virtual reconstruction of the facial nerve course can provide a more comprehensive and immediate understanding of the anatomical relationship between the tumor and the facial nerve, even for surgeons unaccustomed to DESS-WE-MRI images.

One thing to note is the diagnostic performance of DESS-WE-MRI images. A recent study along with our data (unpublished) revealed that DESS-WE-MRI was highly effective for visualization of the facial nerve in patients with parotid tumor [15]. With this technique, tumor localization was more reliable than conventional indirect methods. Although distal (peripheral) branches of the facial nerve often could not be visualized, the main trunk was consistently identified. This is critical, because identification of the main trunk of the facial nerve is the first step in preserving the facial nerve during pa-

rotidectomy (antegrade dissection of the facial nerve) [8,9].

Preoperative simulations using 3D reconstruction techniques are becoming popular with advancement of technology in image processing and computer performance. The technique requires a correct volume of interest to accurately reconstruct a target organ, and has been mainly applied to cases with a clearly demarcated anatomical boundary, such as the facial bone, bronchus, or thyroid gland [16-19].

In contrast, imaging of the peripheral nerve or facial nerve seems to be technically challenging. It was difficult to apply 3D modeling to visualize the facial nerve in the parotid gland because the facial nerve and the branches are very thin and are not clearly distinguished from the gland in conventional MRI images. In addition, the facial nerve in the parotid gland has many anatomical variations in its course, both physiologically and pathologically. In spite of these technical difficulties, facial nerve tracing within the parotid gland using a DESS-WE-MRI can afford us more realistic (accurate) 3D reconstruction of the facial nerve for preoperative surgical planning of the parotid tumors.

There are some issues to be resolved with our method. The regions of interest (the facial nerve and the tumor) were extracted manually through the differences in the signal intensity on the DESS-WE-MRI images. It is a laborious and time-consuming task that needs to identify and select the corresponding anatomic structures on each image slice by the researcher. Artificial intelligence technology or machine learning algorithms might be used for this purpose [20].

In summary, we presented for the first time 3D reconstruction of the facial nerve in two patients with parotid gland tumor by using DESS-WE-MRI, which allowed the surgeon to make better surgical plans for preservation of the facial nerve. This method may contribute to clinical improvement of the outcomes of parotidectomy, particularly in complicated cases.

CONFLICTS OF INTEREST

No potential conflict of interest relevant to this article was reported.

ACKNOWLEDGMENTS

This work was supported by the Haengdan Research Grant of Sungkyunkwan University (No. S-2020-1181-000).

ORCID

Yong Gi Jung https://orcid.org/0000-0001-7456-849X
Yi-Kyung Kim https://orcid.org/0000-0002-9395-4879
Hyung-Jin Kim https://orcid.org/0000-0003-3576-3625
Han-Sin Jeong https://orcid.org/0000-0003-4652-0573

AUTHOR CONTRIBUTIONS

Conception or design: HSJ.
Acquisition, analysis, or interpretation of data: YGJ, YKK, HJK.
Drafting the work or revising: YGJ, HJK, HSJ.
Final approval of the manuscript: YGJ, YKK, HJK, HSJ.

REFERENCES

1. Pinkston JA, Cole P. Incidence rates of salivary gland tumors: results from a population-based study. Otolaryngol Head Neck Surg 1999;120:834-40.
2. O'Brien CJ. Current management of benign parotid tumors: the role of limited superficial parotidectomy. Head Neck 2003;25:946-52.
3. Bron LP, O'Brien CJ. Facial nerve function after parotidectomy. Arch Otolaryngol Head Neck Surg 1997;123:1091-6.
4. Dulguerov P, Marchal F, Lehmann W. Postparotidectomy facial nerve paralysis: possible etiologic factors and results with routine facial nerve monitoring. Laryngoscope 1999;109:754-62.
5. Eisele DW, Wang SJ, Orloff LA. Electrophysiologic facial nerve monitoring during parotidectomy. Head Neck 2010;32:399-405.
6. Guntinas-Lichius O, Gabriel B, Klussmann JP. Risk of facial palsy and severe Frey's syndrome after conservative parotidectomy for benign disease: analysis of 610 operations. Acta Otolaryngol 2006;126:1104-9.
7. Jin H, Kim BY, Kim H, Lee E, Park W, Choi S, et al. Incidence of postoperative facial weakness in parotid tumor surgery: a tumor subsite analysis of 794 parotidectomies. BMC Surg 2019;19:199.
8. Pather N, Osman M. Landmarks of the facial nerve: implications for parotidectomy. Surg Radiol Anat 2006;28:170-5.
9. Rea PM, McGarry G, Shaw-Dunn J. The precision of four commonly used surgical landmarks for locating the facial nerve in anterograde parotidectomy in humans. Ann Anat 2010;192:27-32.

10. Ariyoshi Y, Shimahara M. Determining whether a parotid tumor is in the superficial or deep lobe using magnetic resonance imaging. J Oral Maxillofac Surg 1998;56:23-6.
11. Divi V, Fatt MA, Teknos TN, Mukherji SK. Use of cross-sectional imaging in predicting surgical location of parotid neoplasms. J Comput Assist Tomogr 2005;29:315-9.
12. Ishibashi M, Fujii S, Kawamoto K, Nishihara K, Matsusue E, Kodani K, et al. The ability to identify the intraparotid facial nerve for locating parotid gland lesions in comparison to other indirect landmark methods: evaluation by 3.0 T MR imaging with surface coils. Neuroradiology 2010;52:1037-45.
13. Fujii H, Fujita A, Yang A, Kanazawa H, Buch K, Sakai O, et al. Visualization of the peripheral branches of the mandibular division of the trigeminal nerve on 3D double-echo steady-state with water excitation sequence. AJNR Am J Neuroradiol 2015;36:1333-7.
14. Qin Y, Zhang J, Li P, Wang Y. 3D double-echo steady-state with water excitation MR imaging of the intraparotid facial nerve at 1.5T: a pilot study. AJNR Am J Neuroradiol 2011;32:1167-72.
15. Fujii H, Fujita A, Kanazawa H, Sung E, Sakai O, Sugimoto H. Localization of parotid gland tumors in relation to the intraparotid facial nerve on 3D double-echo steady-state with water excitation sequence. AJNR Am J Neuroradiol 2019;40:1037-42.
16. Beaumont T, Ideias PC, Rimlinger M, Broggio D, Franck D. Development and test of sets of 3D printed age-specific thyroid phantoms for ^{131}I measurements. Phys Med Biol 2017;62:4673-93.
17. Chan HH, Siewerdsen JH, Vescan A, Daly MJ, Prisman E, Irish JC. 3D rapid prototyping for otolaryngology-head and neck surgery: applications in image-guidance, surgical simulation and patient-specific modeling. PLoS One 2015;10:e0136370.
18. Speggiorin S, Durairaj S, Mimic B, Corno AF. Virtual 3D modeling of airways in congenital heart defects. Front Pediatr 2016;4:116.
19. Kirke DN, Owen RP, Carrao V, Miles BA, Kass JI. Using 3D computer planning for complex reconstruction of mandibular defects. Cancers Head Neck 2016;1:17.
20. Ren X, Xiang L, Nie D, Shao Y, Zhang H, Shen D, et al. Interleaved 3D-CNNs for joint segmentation of small-volume structures in head and neck CT images. Med Phys 2018;45:2063-75.